鳥取大学研究成果リポジトリ
Tottori University research result repository

タイトル Title	Enhancement of Catalytic Activity for Toluene Disproportionation by Loading Lewis Acidic Nickel Species on ZSM-5 Zeolite
著者 Auther(s)	Suganuma, Satoshi; Nakamura, Koshiro ; Okuda, Akihito; Katada, Naonobu
掲載誌・巻号・ページ Citation	Molecular catalysis , 435 : 110 - 117
刊行日 Issue Date	2017
資源タイプ Resource Type	学術雑誌論文 / Journal Article
版区分 Resource Version	著者版 / Author
権利 Rights	Copyright © 2017 Elsevier B.V. All rights reserved. This manuscript version is made available under the CC-BY-NC-ND 4.0 license https://creativecommons.org/licenses/by-nc-nd/4.0/
DOI	10.1016/j.mcat.2017.03.029
URL	http://repository.lib.tottori-u.ac.jp/5728

1 **Enhancement of Catalytic Activity for Toluene Disproportionation by Loading**

2 **Lewis Acidic Nickel Species on ZSM-5 Zeolite**

3 Satoshi Suganuma*[1], Koshiro Nakamura[2], Akihito Okuda[2], and Naonobu Katada[2]

4 1 Center for Research on Green Sustainable Chemistry, Graduate School of Engineering,

5 Tottori University, 4-101 Koyama-cho Minami, Tottori 680-8552, Japan

6 2 Department of Chemistry and Biotechnology, Graduate School of Engineering, Tottori

7 University, 4-101 Koyama-cho Minami, Tottori 680-8552, Japan

8 * E-mail: suganuma@chem.tottori-u.ac.jp, Tel.: +81 (857) 31-5256, Fax: +81 (857)
9 31-5684

10

11 **Abstract**

12 Impregnation of various heteroelements on the ZSM-5 zeolite was applied to

13 improvement of the catalytic activity in toluene disproportionation.   Nickel loaded on

14 ZSM-5 (Ni/ZSM-5) exhibited higher catalytic activity (toluene conversion) and lower

15 benzene / xylene ratio (closer to the stoichiometry, meaning low rate of side reaction)

16 than H-ZSM-5 zeolite.   The Ni/ZSM-5 with Ni/Al = 0.6 showed the maximum in

17 catalytic activity, and excess Ni loading caused decrease in the conversion and increase

18 in the benzene / xylene ratio due to decrease of acid amount and acceleration of

19 dealkylation, respectively.   The detailed analysis of acidic property by means of

1   ammonia IRMS-TPD method showed that the Ni loading generated Lewis acid sites on

2   the zeolite.　 The synergy of Brønsted and Lewis acid sites, ascribed to Si-OH-Al and

3   Ni species, respectively, is suggested to give the high activity of desired reaction.

4

7

8   **1.　 Introduction**

9   *Para*-xylene is one of the most valuable aromatic compounds, because it is the

10   raw material of polyethylene terephthalate.　 The selective formation of *para*-xylene is

11   performed in the toluene disproportionation (Scheme S1 in the supporting information),

12   as well as the alkylation of toluene with methanol, the transalkylation of methylbenzene

13   derivatives and xylene isomerization.　 In toluene disproportionation, a ZSM-5 zeolite

14   with the micropores whose size is similar to the benzene ring is utilized as a catalyst

15   forming *para*-xylene selectively [1,2].　 Recent studies concerns with the modification

16   of ZSM-5 to improve the selectivity of *para*-xylene, including impregnation of P, Mg, B

17   and La [3-5], pre-coking [6,7], chemical vapor deposition (CVD) [8,9], chemical liquid

18   deposition (CLD) of silica [10-12], and silicalite coating [13].　 The selectivity of

19   *para*-xylene 93% in the C8 aromatic compounds at 30% of the toluene conversion in

1 the industrial process has been achieved [14]; the selectivity is usually decreased with

2 increasing the conversion by varying the reaction conditions on one catalyst, and

3 therefore the high selectivity at a certain high level of conversion is demanded. The

4 99.8% selectivity at 10.9% of the conversion have been achieved in laboratory [15].

5 Further improvement of the catalyst available to industrial process is strongly demanded,

6 because the energy-consuming separation step after the reaction can be omitted with

7 such a high selectivity over 99.7 %. Two alternatives can be proposed to realize the

8 high performance, (1) suppression of the undesired reaction presumably due to

9 heterogeneous pore-opening size, or (2) enhancing the catalytic activity of zeolite.

10 Attempts from the former viewpoint have been carried out based on various techniques

11 [6-13]. The present study focuses on the latter concept. Modification of the active

12 sites in the ZSM-5 is attempted to increase the activity.

13 In this study, we selected the sample of ZSM-5 (MFI structure) with the

14 practically highest Al concentration (SiO_2 / Al_2O_3 = 23.8) as the parent zeolite because

15 of the following reasons. (1) The MFI structure possessed the shape selectivity in

16 toluene disproportionation. (2) The active species for this reaction has been generally

17 considered to be Brønsted acid site [10]. The number of Brønsted acid sites on

18 zeolites is principally equal to the number of Al atoms [16].

1   In the present study, we introduced various heteroelements on the ZSM-5 zeolite

2 to improve the catalytic activity, because this method was assumed to keep the pore

3 structure of the zeolite. We investigated the catalytic activity and the reaction

4 mechanism for the toluene disproportionation of heteroatoms supported on ZSM-5 with

5 the high Al concentration.

6

7 **2. Experimental**

8   A Na/ZSM-5 (Tosoh, SiO_2 / Al_2O_3 = 23.8) zeolite was ion-exchanged into

9 NH_4-ZSM-5 in an 5 wt.% ammonium nitrate solution (NH_4 / Na in the system = 10) at

10 353 K for 4 h, then filtrated and washed with water 3 times. These procedures (stirring,

11 filtrating and washing) were repeated 3 times. The zeolite finally was dried at 373 K for

12 12 h. The thus obtained NH_4-form zeolite was employed as the parent zeolite in the

13 following modification procedures without converting it into the proton form, because it

14 has been known that proton form zeolites can be dealuminated by water vapor in

15 atmosphere [17,18].

16   The introduction of nickel and other metals were typically performed by means

17 of an impregnation method. 100 mL of aqueous nitrate solution of the metal elements

18 were impregnated on 5.0 g of NH_4-ZSM-5 with stirring at 353 K. Then, the solvent

1   was dried at 373 K for 12 h in air. The yielded solid is named Ni-x where x is the Ni/Al

2   molar ratio based on the composition of impregnated solution; the metal to Al ratio was

3   fixed at 0.6 in the cases of other metals. A Ni/SiO$_2$ catalyst with 6.1 wt% of Ni was also

4   prepared by the same method using a silica gel support (Reference Catalyst, Catalysis

5   Society of Japan, JRC-SIO-10).   As a comparison, a sample of Ni/ZSM-5 was

6   prepared by means of an ion exchange method.   After the ZSM-5 zeolite was put into

7   an aqueous solution of nickel nitrate and stirred at 353 K for 4 h, the solid was filtered

8   and dried at 373 K for 12 h in air.   The yielded solid is named Ni-x(EX) where x is the

9   Ni/Al molar ratio based on the composition of employed solution, and the actual

10   composition was measured by ICP as described later.

11   The crystal structure was characterized by X-ray diffraction (Rigaku, Ultima IV),

12   inductively coupled plasma-atomic emission spectrometry (Rigaku, ICP CIROS), and

13   N$_2$ adsorption (Microtrac BEL, BELSORP-MAX).   The adsorption isotherms was

14   measured at 77 K after pretreatment at 573 K, and the surface area and the pore volume

15   were   calculated   based   on   BET   (Brunauer-Emmett-Teller)   equation,   BJH

16   (Barrett-Joyner-Halenda), and t-plot methods.

17   Ammonia IRMS-TPD analysis [19] was carried out using an automatic

18   IRMS-TPD analyzer (MicrotracBEL).   Powder of Ni/ZSM-5 was compressed into a

1   self-supporting disk with 1 cm of the diameter under 20 MPa, and pre-treated in an

2   oxygen flow (37 μmol s^{-1}, 100 kPa) at 823 K for 1 h and a hydrogen flow (7 μmol s^{-1},

3   100 kPa) at 773 K for 1 h in an in-situ IR cell.   Also NH$_4$-ZSM-5 was pre-treated in

4   similar way into H-ZSM-5, but the hydrogen treatment was omitted.   The sample was

5   heated at a ramp rate of 2 K min^{-1} during the elevation temperature from 343 to 803 K

6   in a helium flow (89 μmol s^{-1}, 6.0 kPa), and an IR spectrum was collected.   Then,

7   ammonia was adsorbed at 343 K, and the heating and collecting IR spectra in a helium

8   flow were repeated.   The concentration of ammonia in the gas phase was monitored by

9   a mass spectrometer (MS) operating at m/e 16. The amount of acid sites was calculated

10   from the intensity of ammonia desorption in the TPD spectrum.   The enthalpy of

11   ammonia desorption (ΔH) was calculated as an index of acid strength from the ammonia

12   desorption profile based on the thermodynamic theory [20].

13   Nickel on ZSM-5 was characterized by means of IR spectroscopy of adsorbed

14   CO using an automatic IRMS-TPD analyzer (MicrotracBEL).   The catalysts was

15   pretreated at 823 K in an oxygen flow and in a hydrogen flow.   Then, the IR cell was

16   cooled to 293 K, and evacuated.   The background was recorded in evacuation at 293 K.

17   After introduction of CO, the IR cell was evacuated for 15 min.   IR spectra in each

18   step was recorded at every predetermined time.   The CO adsorption capacity was

1 analyzed by a volumic gas adsorption analyzer (Microtrac BEL, BELSORP-MAX).

2 The samples were pre-treated in an oxygen flow at 773 K for 1 h and a hydrogen flow at

3 773 K for 1 h in an in-situ sample tube. CO was adsorbed on the samples at 323 K.

4 In order to evaluate the activity for the toluene disproportionation, 0.1 g of the

5 catalyst was packed in a stainless steel tube (i.d. 4 mm) and pretreated in H_2 (0.015 mol

6 h^{-1}, 100 kPa) at 773 K for 1 h. In this process, ammonium ion on the zeolite was

7 desorbed, and H(proton)-type zeolite was formed. Then, the catalyst bed was cooled

8 down to 673 K, and the back-pressure valve was adjusted to keep the total pressure at

9 1.5 MPa. Toluene and H_2 were fed at 0.015 mol h^{-1} for each. The products were

10 trapped by hexane at 273 K and analyzed by a GC (gas chromatograph) with a FID

11 (flame ionization detector). On the other hand, dealkylation (cracking) of cumene

12 (isopropylbenzene, 2-phenylpropane) was carried out by a pulse method in a He flow as

13 described elsewhere [21]. The catalyst (1 mg) was packed in a stainless steel tube (i.d. 4

14 mm) and pretreated in a He flow (0. 15 mol h^{-1}, 100 kPa) at 773 K for 1 h. Then, a pulse

15 of cumene (28.7 μmol) was fed at 473 K. The outlet gas was analyzed by a GC (gas

16 chromatograph) with a FID (flame ionization detector).

17

18 **3. Results**

3.1. Characterization of Ni/ZSM-5

The structural analyses were applied to Ni/ZSM-5 (Ni-0.6, Ni-1.0 and Ni-2.1) and H-ZSM-5. It is presumed that Ni species before the reaction had been fully oxidized and dispersed on surface, because they were formed from nickel nitrate solution. The pretreatment of reaction was carried out in a flow of H_2, and Ni species should be reduced. Fig. 1 (a) displays X-ray diffraction patterns of the catalysts after the reduction in a flow of H_2 at 773 K for 1 h. The patterns of Ni/ZSM-5 exhibited narrowed and well-defined diffraction peaks similar to those of H-ZSM-5, demonstrating that the crystal structure of MFI structure in the Ni/ZSM-5 were unchanged by the Ni loading and H_2 reduction. Fig. 1 (b) shows an enlarged portion of Fig. 1 (a). The XRD patterns of Ni/ZSM-5 revealed clear additional peaks at $2\theta =$ 44.5º and 51.8º attributable to Ni metal particles, and the peak was especially large on Ni-2.1.

The Ni/Al molar ratios in the catalysts were determined by ICP analysis, as shown in Table 1. The Ni/Al contents in Ni-0.6 and Ni-1.0 prepared by the impregnation method were found to be in generally agreement with the composition of impregnated solutions, indicating that most of Ni was loaded on the support by the impregnation procedure. On the other hand, Ni-0.5(EX) and Ni-0.9(EX) were

1 prepared by the ion-exchange method, where the zeolite and solution were stirred at the

2 same temperature employed for the impregnation method and then unfixed Ni was

3 washed out. Most of Ni was loaded on Ni-0.5(EX) as confirmed by ICP. However,

4 the ICP analysis for Ni-0.9(EX) indicated that only 0.56 of Ni relative to Al was

5 exchanged while 0.90 of Ni was employed. In other words, the ion exchange capacity

6 of Ni on this NH_4-ZSM-5 in these conditions was about a half of Al content. This

7 suggests that the valence of Ni was two during the ion exchange procedure. The

8 employed H-ZSM-5 (SiO_2 / Al_2O_3 = 23.8) had 1.29 mol kg^{-1} of Al and 6.1 wt% of

9 nickel represented 1.04 mol kg^{-1}, considering that nickel (Ni^{2+}) could undergoes

10 exchange in one or two acid sites. This means that 4.2 wt% is the superior limit for

11 exchange nickel. For instance Ni-0.9(EX) and Ni-0.5(EX) show similar Ni/Al ratio.

12 As shown in Fig. 2, N_2 adsorption-desorption isotherms of the investigated

13 samples were of type I, evidencing a microporous texture. In addition, presence of the

14 slope at P/P_0 = 0.4 - 1 (clearly shown by the presence of hysteresis loop) in the each

15 isotherm suggests mesoporous feature. The uptake at P/P_0 close to zero was almost

16 unchanged by the Ni loading, consistent with the microporous structure was not

17 modified by the Ni impregnation procedure. Surface area of micropore and larger pore

18 wall remained approximately invariable (Fig. S1). Pore volume of micropore was the

1   same in the catalysts, while that of mesopore increased by Ni loading (Fig. S2).

2   The acidic properties of Ni/ZSM-5 and H-ZSM-5 were analyzed by a method of

3   ammonia   infrared-mass   spectroscopy   /   temperature-programmed   desorption

4   (IRMS-TPD).   This method can determine the number, strength (enthalpy or energy of

5   ammonia desorption) and type (Brønsted or Lewis) of acid sites on a solid [16].   Fig. 3

6   shows enlarged portions of difference IR spectra obtained on the zeolites at 373-773 K

7   during the TPD experiments.   A sharp band at ca. 1450 cm^{-1} was assigned to bending

8   (v_4) vibration of NH_4^+ adsorbed on Brønsted acid sites (NH$_4$B).   This band was

9   observed even after the loading of Ni with more than 2 of the Ni/Al ratio, demonstrating

10   that a fraction of Brønsted acid sites were not interacted with Ni cation.   It is supposed

11   that the impregnated Ni^{2+} species were partially transformed in the process of

12   pretreatment (reduction by H_2) into metal particle which indirectly or not interacted with

13   the support, and therefore Brønsted acid site was regenerated.   A small peak at ca.

14   1622 cm^{-1} was attributed to δ_d of NH$_3$L (NH$_3$ coordinated to Lewis acid sites) [20].   On

15   pure aluminosilicates with Lewis acidity due to Al species, a stronger vibration mode

16   (δ_s) is observed at 1250-1330 cm^{-1}, and the intensity changes against the temperature of

17   δ_d and δ_s are similar, because these bands are two different modes of one compound.

18   The amount of NH$_3$L (ammonia coordinated to Lewis acidic Al species in the case of

10

1   aluminosilicate) was calculated from the IR-TPD of δ_s, in order to minimize the error

2   utilizing the more intense band [19].   However, the intensities of δ_d and δ_s are not

3   consistent in Ni/ZSM-5, suggesting the presence of hidden band of δ_s.   It is considered

4   that the band of δ_s on Ni/ZSM-5 had a lower wavenumber than that on aluminosilicate,

5   and was thus overlapped by the skeletal vibration of zeolites; it is reasonable that the

6   NH_3-Ni species has a different vibration frequency from that of NH_3-Al.   The amount

7   of NH_3L was determined from IR-TPD of δ_d.   The peak ascribed to NH_3L was not

8   observed in the spectra of H-ZSM-5 (Fig. 3 (a)), and the loading of Ni created Lewis

9   acid sites (Fig. 3 (b)-(d)).   The peak around 1680 cm^{-1} in all the spectra was ascribed to

10   the δ_s vibration of NH_3 hydrogen-bonded [19].

11   Fig. 4 shows TPD profiles of ammonia desorbed from the acid sites.   MS-TPD

12   indicates the profile of NH_3 desorption evaluated with mass spectroscopy.   The TPD

13   profiles of NH_4B and NH_3L were calculated from the IR-TPD of ca. 1450 cm^{-1}-band (ν_4,

14   NH_4) and ca. 1622 cm^{-1}-band (δ_d, M-NH_3), respectively.   MS-TPD was assumed to be

15   the sum of TPD profiles for NH_4B and NH_3L, while the peak around 410 K was

16   ascribed to NH_3 hydrogen-bonded and was not contained as species adsorbed on acid

17   sites.   Table 2 lists the acid amount and average enthalpy upon NH_3 desorption (ΔH,

18   index of acid strength) calculated from the TPD profiles.   It was found that the loading

1   of Ni decreased the Brønsted acid sites and increased the amount of Lewis acid sites.

2   The strength (ΔH) of Brønsted acid sites slightly declined by Ni-loading.   On the other

3   hand, average ΔH of Lewis acid sites cannot appropriately calculated, because TPD

4   profiles for NH_3L were much broader than those for NH_3B.

5   Many researchers reported CO adsorption on different nickel species, and

6   especially Hadjiivanov et.al. studied FTIR analysis of CO adsorption on Ni/ZSM-5 [22]

7   and Ni/SiO_2 [23].   CO adsorbed on oxidized Ni/ZSM-5 was mainly bonded with Ni^{2+}

8   by a σ bonding [22].   After reduction of Ni/ZSM-5, a fraction of nickel species were

9   changed into Ni^+, which were bonded with CO by π-back bonding [22].   CO bonded

10   with acidic hydroxyls on zeolite was also detected on Ni/ZSM-5 [22].   CO adsorbed on

11   reduced Ni/SiO_2 was characterized as polycarbonyl coordinated with nickel metal [23].

12   In our study, the samples were pretreated in flow of hydrogen at 773 K, and then cooled

13   to 293 K.   The background spectrum was recorded in evacuation.   After introduction

14   of CO (about 3 kPa equilibrium pressure), CO was evacuated for 15 minutes.   Fig. S3

15   shows IR spectra in the process of CO desorption on the catalysts.   The wavenumber

16   of the stretching vibration of CO gas is 2143 cm^{-1}.   In Fig. S3 (a), the bands at 2170

17   and 2121 cm^{-1} were assigned to H-bonded CO and physically adsorbed CO on

18   H-ZSM-5, respectively.   The bands at 2209 and 2054 - 2050 cm^{-1} on Ni-0.6 and Ni-1.0

1   (Fig. S3 (b) and (c)) were also observed, and assigned to monocarbonyl of Ni^{2+} - CO

2   type [22] and tetracarbonyl of Ni^0 $(CO)_4$ type [23].   The weak bands at 2100-2090 and

3   2003 cm^{-1} may be assignable to $Ni(CO)_4$ of defect sites and Ni^0 $(CO)_x$ $(x < 4)$,

4   respectively.   Namely, CO introduced into Ni-0.6 and Ni-1.0 was adsorbed on Ni^{2+}, Ni^0

5   metal, and acidic hydroxyl group.   In Fig. S3 (d), CO introduced into Ni-2.1 was

6   adsorbed on Ni^0 metal and acidic hydroxyl group.   The shoulder band at 2087 cm^{-1}

7   may be assignable to $Ni(CO)_4$ of defect sites, and the broad band at 1901 cm^{-1} was

8   speculated to be assigned to $Ni^0{}_x(CO)$ $(x > 1)$ [23].   Nickel on Ni-2.1 is not Ni^{2+} but

9   Ni^0 metals, which aggregate speculatively.   It was revealed that the low content of Ni

10   on the catalyst kept oxidation state of nickel.   Fig. S4 shows amount of adsorbed CO at

11   323 K.   The large amount of loading nickel (Ni / Al > 0.6) leaded gradual increase in

12   the amount of adsorbed CO.

13

14   **3.2. Catalytic activity for toluene disproportionation**

15   Various transition metals were introduced into ZSM-5 at 0.6 of the metal/Al

16   atomic ratio by the impregnation method.   The catalytic activities of the ZSM-5

17   zeolites with different metals for toluene disproportionation were recorded, as shown in

18   Fig. S5, which compares the initial catalytic activity, represented by the conversion at

1   75 min of the time on stream (the initial products were collected between 45 – 75 min,

2   because the influent could not be obtained in the trap tube between 0 – 45 min).   In this

3   reaction, main products were xylene isomers and benzene.   Little other products

4   containing ethylbenzene were detected in FID–GC analysis.   The loading of Ni

5   increased the initial activity by 1.6 times against H-ZSM-5, whereas the other elements

6   decreased the activity.

7   Fig. 5 (a) compares the activities for the toluene disproportionation over

8   Ni/ZSM-5 with various Ni contents; the Ni content is based on the composition of

9   impregnated solution, and this value has been confirmed by ICP to be approximately

10   same to the Ni content in the solid.   The activity increased with the loading in 0 - 1 of

11   the Ni/Al ratio, and showed the maximum at 1.0 of the Ni/Al ratio.   However, excess

12   Ni gave decrease in the activity.   The catalytic activity of Ni/SiO_2 containing the Ni

13   content (6.1 wt%) same to that of Ni-1.0 is shown in Table 3; Ni/SiO_2 exhibited lower

14   conversion than Ni-1.0, but higher than H-ZSM-5 (Ni/Al = 0).

15   The disproportionation of toluene into benzene and xylene should result in

16   unity of the benzene / xylene molar ratio according to the stoichiometry (Scheme S1).

17   The yield of xylene isomers generally showed 26 % *p*-xylene, 53 % *m*-xylene and 21 %

18   *o*-xylene, which are same to the ratios of equilibrium mixture of xylenes.   In this study,

14

1   the shape selectivity was not found as observed on H-ZSM-5 zeolite at a high

2   conversion of toluene without catalyst modification techniques [3-13]. Fig. 5 (b)

3   shows the relationship between the benzene / xylene ratio and Ni content on the ZSM-5

4   support. The benzene / xylene ratio was around 1 at Ni/Al < 1 and increased with

5   loading of excess Ni. The high benzene / xylene ratio indicates the side reaction such

6   as dealkylation of toluene and alkylbenzene (e.g., ethylbenzene). In detail, the

7   benzene / xylene ratio was slightly higher than 1 (ca. 1.2) at Ni/Al = 0 and obviously

8   decreased with Ni loading up to Ni/Al = 0.6. On the other hand, Ni/SiO_2 showed an

9   obviously high value, 14.3, of the benzene / xylene ratio in the same reaction conditions,

10   suggesting that the Ni^0 particle on Ni/SiO_2 generated high dealkylation activity.

11   Fig. 6 shows the catalytic activity for cumene cracking, which has been utilized

12   as a test reaction of solid acid catalyst. It also revealed the maximum at 1.0 of the

13   Ni/Al ratio, similarly to the toluene disproportionation. These suggest that the Ni/Al

14   ratio 1 was effective in the enhancement of activity, and the excess Ni induced drastic

15   decline of the catalytic activity.

16   Fig. 7 (a) shows the toluene conversion as a function of time on stream in the

17   toluene disproportionation. Besides the activity change by Ni loading stated above,

18   the conversion of Ni loaded on ZSM-5 zeolites and Ni/SiO_2 was gradually decreased

1 with the time on stream, and showed a plateau over 240 min. The catalytic activities

2 of Ni-0.6 and Ni-1.0 even after decline exhibited higher than that of H-ZSM-5. On the

3 other hand, Ni/SiO$_2$ and Ni-2.1 seems to have very high initial activity but showed

4 relatively fast decrease of the conversion. Ni-0.6 exhibited comparable stability to

5 H-ZSM-5. Fig. 7 (b) compares the benzene/xylene molar ratio as a function of the

6 time on stream. As already stated, Ni-0.6 showed the benzene / xylene ratio lower

7 than that on H-ZSM-5. The benzene/xylene ratios for Ni/SiO$_2$ showed >13.0 over the

8 time on stream in the present experiments (data not shown).

9

10 **4. Discussion**

11 **4.1. Characterization**

12   According to Maia et al. [24], Ni-ZSM-5 prepared by impregnation and

13 calcination in air has three types of nickel species; NiO particle, nickel oligomeric

14 species in the zeolite channels, and nickel species as the counter cations of ion exchange

15 sites in the zeolite framework. In the TPR (temperature-programmed reduction)

16 profiles, nickel species in NiO particle are reduced at temperature lower than those

17 required for reducing nickel oligomeric species in the zeolite channels. It is

18 considerably difficult to reduce nickel species as counter cations in the zeolite

1   framework.

2   The chemical compositions of ion exchanged samples suggested that the ion

3   exchange capacity of the employed ZSM-5 was about a half of Al content at 353 K, the

4   temperature commonly adopted to the ion exchange and impregnation methods,

5   presumably because that Ni was divalent.   It implies that most of Ni species on Ni-0.6

6   were the counter cations of ion exchange sites (hereafter counter cation); the

7   pretreatment of reaction may reduce all or a part of them, but anyway, finely dispersed

8   Ni species were presumably formed on Ni-0.6, simultaneously the Brφnsted acid sites

9   were reproduced.   In the ICP analysis (Table 1), it indicates that 0.56 – 0.57 of Ni

10   relative to Al can be loaded on the zeolite.   In the impregnation process, most of Ni

11   species should be divalent and loaded as the counter cations of two ion exchange sites.

12   However, all ion exchange sites on the ZSM-5 zeolite do not possess adjacent another

13   ion exchange sites.   The isolated site may possess one Ni counter cation, which cause

14   that ion-exchange capacity by Ni is 0.56 – 0.57.   On the contrary, it is speculated that

15   the surplus of Ni preferentially formed oligomeric species in the zeolite channels in the

16   cases where the amount of such Ni species was small.   It is therefore considered that

17   Ni-0.6 mainly possessed the counter cations-originated species, whereas Ni-1.0 had

18   both of the counter cations-originated species and the oligomerized species in zeolite

1   channels.   The driving force of dispersion of these species should be the presence of

2   ion exchange sites and microporous nature, and therefore most of Ni species in these

3   samples are considered to be located in the micropores nearby acidic OH groups (ion

4   exchange sites).   On the contrary, excess Ni should be weakly attached to the surface

5   in the cases of impregnation method, and therefore it is speculated that relatively large

6   fractions of Ni in Ni-2.1 formed particles on the external surface as aggregates.   Nickel

7   in Ni/SiO_2 was probably reduced into Ni particle far larger than atomic scale.

8   As shown in Table 2, the loading of Ni up to 1 of Ni/Al ratio decreased the

9   Brønsted acid sites and increased the amount of Lewis acid sites.   Therefore, the

10   modification of acidic property by Ni loading can be summarized as follows: [i]

11   Brønsted acid site was decreased by ion exchange with Ni species, and [ii] Lewis acid

12   sites were generated on relatively small Ni particles dispersed in the zeolite channels.

13

14   **4.2. Catalytic activity**

15   The enhancement of activities for both reactions (cumene cracking and toluene

16   disproportionation) is considered to be due to generation of the nickel species and some

17   changed of Brønsted acidic nature of ZSM-5.   In toluene disproportionation, the

18   activity was found to be increased with loading of Ni up to 1 of Ni/Al ratio, suggesting

1 that co-presence of the relative dispersed Ni species in the zeolite channels and the

2 ion-exchange sites generated the activity.   Benzene / xylene ratio of Ni-0.6 showed

3 close to 1, which was lower than that of Ni-0.5.   The appropriate loading amount was

4 0.6.

5   In contrast, the excess Ni loaded on the ZSM-5 zeolite (Ni/Al > 1.0) is

6 considered to catalyze side reaction and show high benzene/xylene ratio, as well as that

7 on the silica gel.   It suggests that the reduced Ni species derived from NiO particle in

8 Ni/SiO$_2$ have intrinsically high conversion of toluene and benzene / xylenes ratio.   Fast

9 deactivation was observed on Ni-2.1 and Ni/SiO$_2$.   These are reasonably consistent

10 with each other, because the side reaction forming benzene and alkenes should increase

11 the benzene / xylene ratio and simultaneously increase the rate of coke formation from

12 alkenes, resulting in the catalyst deactivation.   The appropriate amount of Ni loading to

13 form the Ni species dispersed in the zeolite channels to keep the synergy with ion

14 exchange sites is believed to enhance the catalytic activity for toluene

15 disproportionation, and improved the xylene selectivity.

16

17 **4.3. Reaction mechanism**

18   Some preceding studies proposed the reaction mechanisms of toluene

1 disproportionation based on the experimental observations (Scheme S2) [25-27]. The

2 mechanism drawn in Scheme S2 [26] proceeds through hydride abstraction followed by

3 the formation of diphenyl methane; these steps were accelerated by Brønsted and Lewis

4 acid sites.

5   This study suggested that the Ni-0.6 sample possessed Ni species as counter

6 cations (-ONi) in the micropores and showed high catalytic activity and stoichiometric

7 formation of xylene and benzene (1:1). It can be explained that Lewis acid sites

8 derived from –ONi species and the Brønsted acid site on the zeolite worked concertedly

9 to have synergy effect for the toluene disproportionation.   Mavrodinova et al. [28] have

10 suggested that the reactivity of HY zeolite modified with InO^+ was different from a

11 simply Brønsted acidic zeolite, because Lewis acidic InO^+ species lead a faster hydride

12 abstraction and benzylic cation formation upon toluene and ethylbenzene

13 disproportionation.   Recently, it was reported that Pd [29[30]- 31] and Ga [32] anchored

14 on ion-exchange sites of ZSM-5 zeolites generate Lewis acid sites, which act for C-H

15 activation and hydride abstraction. It is probable that the toluene disproportionation

16 for Ni-0.6 proceed with the hydride abstraction enhanced by -ONi as Lewis sites and

17 effective transformation of diphenylmethane-like intermediate by Brønsted acid sites

18 (Scheme S2), resulting in the high toluene conversion and benzene / xylene ratio ≈ 1.

1   This hypothesis is supported by the preceding reports [24,33] that the Ni on Ni/ZSM-5

2   accelerated dehydrogenation in paraffin cracking.

3   Ni particles on Ni-2.1 and Ni/SiO$_2$ brought about faster toluene conversion than

4   Brønsted acid sites on H-ZSM-5, as shown in Table 3.   It is proposed that Ni/SiO$_2$

5   catalyzed side reactions with dealkylation of alkylbenzenes and coking, and hence to

6   result in the rapid catalyst deterioration, as shown in Fig. 7 (a).

7   In this study, the activity of ZSM-5 zeolite for the toluene disproportionation

8   was enhanced by simple impregnation of Ni in mild conditions with keeping the textual

9   properties, unlike hydrothermal treatment.   It is expected that combination of this

10 method and techniques for improvement of *para*-xylene selectivity with control of fine

11 structure which have been developed [10-13, 33] will open a new way to design a

12 catalyst with high selectivity and activity for *para*-xylene production.

13

14 **5. Conclusions**

15 The loading of Ni on ZSM-5 increased the catalytic activity for toluene

16 disproportionation and cumene cracking.   The formed benzene / xylene ratios in

17 toluene disproportionation was improved into nearby 1.0 by the Ni loading content at

18 Ni/Al = 0.6 on ZSM-5.   The MFI crystal structure did not collapse during the Ni

1 loading.   The loading at Ni/Al = 0.6 formed the nickel species as counter cations and

2 Lewis acid sites after the pretreatment in an H_2 flow.   Excessive Ni introduction on the

3 zeolite and loading of Ni on a silica gel generated coarse Ni particles.   The high

4 toluene conversion and the selective xylene for Ni-0.6 were supposed to be ascribed to

5 the synergy effect of Brønsted acid sites and Lewis acid sites.

6

1 **References**

[1] Y.Y. Fong, A.Z. Abdullah, A.L. Ahmad, S. Bhatia, Chem. Eng. J. 139 (2008)

172-193.

[2] S. Al-Khattaf, S.A. Ali, A.M. Aitani, N. Žilková, D. Kubička, J. Čejka, Catal. Rev.

Sci. Eng. 56 (2014) 333-402.

[3] N.Y. Chen, W.W. Kaeding, F.G. Dwyer, J. Am. Chem. Soc. 101 (1979) 6783-6784.

[4] W.W. Kaeding, C. Chu, L.B. Young, B. Weinstein, S.A. Butter, J. Catal. 67 (1981)

159-174.

[5] Y. Sugi, Y. Kubota, K. Komura, N. Sugiyama, M. Hayashi, J.-H. Kim, G. Seo, Appl.

Catal. A 299 (2006) 157-166.

[6] F. Bauer, W.H. Chen, Q. Zhao, A. Freyer, S.B. Liu, Micropor. Mesopor. Mater. 47

(2001) 67-77.

[7] F. Bauer, W.H. Chen, E. Bilz, A. Freyer, V. Sauerland, S.B. Liu, J. Catal. 251 (2007)

258-270.

[8] J.H. Kim, A. Ishida, M. Okajima, M. Niwa, J. Catal. 161 (1996) 387-392.

[9] A.B. Halgeri, J. Das, Catal. Today 73 (2002) 65-73.

[10] J. Čejka, N. Žilková, B. Wichterlova, G. Elder-Mirth, J.A. Lercher, Zeolites 17

(1996) 265-271.

[11] S. Zheng, H. Tanaka, A. Jentys, J.A. Lercher, J. Phys. Chem. B 108 (2004)

1337-1343.

[12] S. Laforge, D. Martin, J.L. Paillaud, M. Gusinet, J. Catal. 220 (2003) 92-103.

[13] D.V. Vu, M. Miyamoto, N. Nishiyama, Y. Egashira, K. Ueyama, J. Catal. 243

(2006) 389-394.

[14] J. S. Beck, D. H. Olson, S. B. McCullen, US Patent 5367099A (1994), to Mobil Oil Corporation.

[15] N. Katada, K. Takeshita, Y. Miyazono, M. Niwa, Y. Araki, Jpn. Patent JP2013-163142A (2013), to Tottori University and Jx Nippon Oil & Energy Corporation.

[16] M. Niwa, N. Katada, K. Okumura, Characterization and Design of Zeolite Catalysts: Solid Acidity, Shape Selectivity and Loading Properties, Springer, Berlin, 2010, p. 29-59.

[17] N. Katada, Y. Kageyama, M. Niwa, J Phys Chem B 104 (2000) 7561-7564.

[18] N. Katada, T. Kanai, M. Niwa, Micropor. Mesopor. Mater. 75 (2004) 61-67.

[19] S. Suganuma, Y. Murakami, J. Ohyama, T. Torikai, K. Okumura, N. Katada, Catal. Lett. 145 (2015) 1904-1912.

[20] M. Niwa, N. Morishita, H. Tamagawa, N. Katada N, Catal. Today 198 (2012) 12-18.

[21] M. Niwa, N. Katada, Y. Murakami, J. Phys. Chem. 94 (1990) 6441-6445.

[22] K. Hadjiivanov, H. Knözinger, M. Mihaynov, J. Phys. Chem. B 106 (2002) 2618-2624.

[23] M. Mihaynov, K. Hadjiivanov, H. Knözinger Catal. Lett. 76 (2001) 59-63.

[24] A.J. Maia, B. Lois, Y.L. Lam, M.M. Pereira, J. Catal. 269 (2010) 103-109.

[25] N. P. Rhodes, R. Rudham, J. Chem. Soc. Faraday Trans. 90 (1994) 809-814.

[26] Y. Xiong, P. G. Rodewald, C. D. Chang, J. Am. Chem. Soc. 117 (1995) 9427-9431.

[27] J. Čejka, B. Wichterlová, Catal. Rev. 44 (2002) 375-422.

[28] V. Mavrodinova, M. Popova, M. R. Mihályi, G. Pál-Borbély, C. Minchev, Appl.

Catal. A 262 (2004) 75-83.

[29] Y. Lou, P. He, L. Zhao, H. Song, Fuel 183 (2016) 396–404.

[30] Y. Lou, J. Ma, W. Hu, Q. Dai, L. Wang, W. Zhan, Y. Guo, X.-M. Cao, Y. Guo, P. Hu, G. Lu, ACS Catal. 6 (2016) 8127–8139.

[31] Y. Lou, P. He, L. Zhao, H. Song, Catal. Commun. 87 (2016) 66–69.

[32] H. Xiao, J. Zhang, X. Wang, Q. Zhang, H. Xie, Y. Hana, Y. Tan, Catal. Sci. Technol., 5 (2015) 4081-4090.

[33] A.J. Maia, B.G. Oliveira, P.M. Esteves, B. Lois, Y.L. Lam, M.M. Pereira, Appl. Catal. A 403 (2011) 58-64.

Table 1   Ni/Al molar ratios in Ni/ZSM-5

Sample	Ni/Al based on the composition of impregnation / ion exchange solution	ICP Ni/Al
Ni-0.5*	0.50	0.57
Ni-1.0*	1.04	1.01
Ni-0.5(EX)**	0.50	0.51
Ni-0.9(EX)**	0.90	0.56

*: Impregnation method.   **: Ion exchange method.

Table 2   Acidic properties of Ni/ZSM-5

| Sample | Brønsted acid site | | Lewis acid site |
| | Amount | ΔH [*1] | Amount |
	/ mol kg^{-1}	/ kJ mol^{-1}	/ mol kg^{-1}
H-ZSM-5	1.13	141	0.00
Ni-0.6	0.78	136	0.54
Ni-1.0	0.58	134	0.83
Ni-2.1	0.51	134	0.67

[*1] Average enthalpy upon NH$_3$ desorption

Table 3   Catalytic activity of various catalysts in toluene disproportionation

Sample	Ni / wt%	Conversion* / %	Benzene / xylene molar ratio*
H-ZSM-5	0	10.8	1.25
Ni-0.6 (Ni/ZSM-5)	3.7	18.3	1.07
Ni-1.0 (Ni/ZSM-5)	6.1	25.5	1.37
Ni-2.1 (Ni/ZSM-5)	12.8	12.3	1.50
Ni/SiO$_2$	6.1	16.4	14.3

*: At time on stream = 75 min.

Figure captions

Fig. 1   (a) XRD patterns and (b) enlarged portion in $2\theta = 40\text{-}60°$.

Fig. 2 N_2 adsorption-desorption isotherms at 77 K.

Fig. 3   Enlarged portion at bending vibration region (1100 – 2000 cm^{-1}) in difference spectra of IR $A(T)$-$N(T)$ [(spectrum after ammonia adsorption) – (spectrum before ammonia adsorption)] on (a) H-ZSM-5, (b) Ni-0.6, (c) Ni-1.0, and (d) Ni-2.1.

Fig. 4   Fitting of IR- and MS-TPD calculating TPD spectrum of Brønsted acid site on (a) H-ZSM-5, (b) Ni-0.6, (c) Ni-1.0, and (d) Ni-2.1.

Fig. 5   (a) Initial conversion of toluene and (b) benzene / xylene molar ratio in disproportionation of toluene on Ni-promoted ZSM-5.

Fig. 6   Initial conversion in dealkylation of cumene on Ni-promoted ZSM-5.

Fig. 7   (a) Conversion of toluene and (b) benzene / xylene molar ratio as a function of time on stream in disproportionation of toluene by Ni/ZSM-5, H-ZSM-5 and Ni/SiO$_2$.
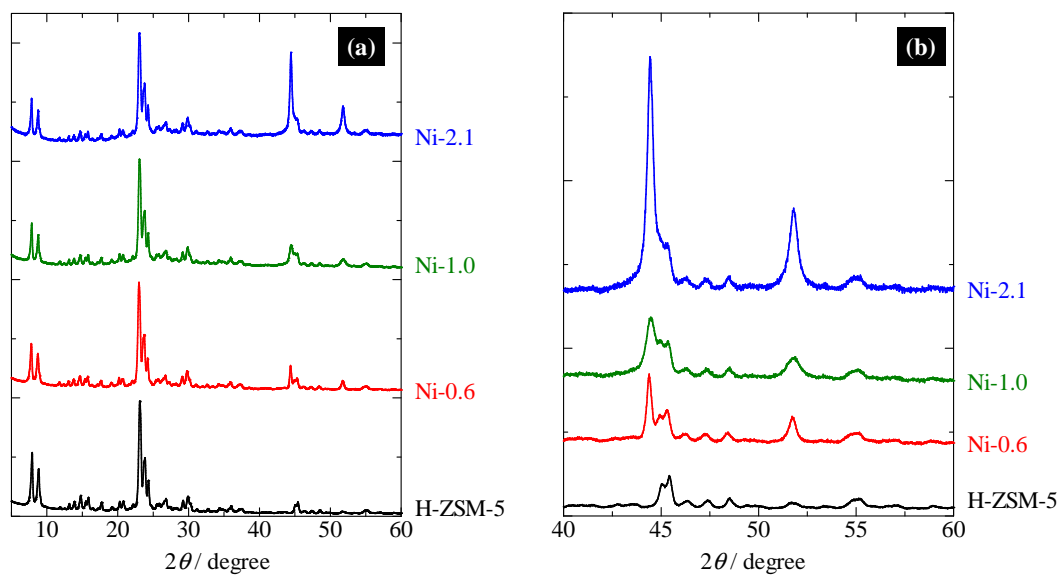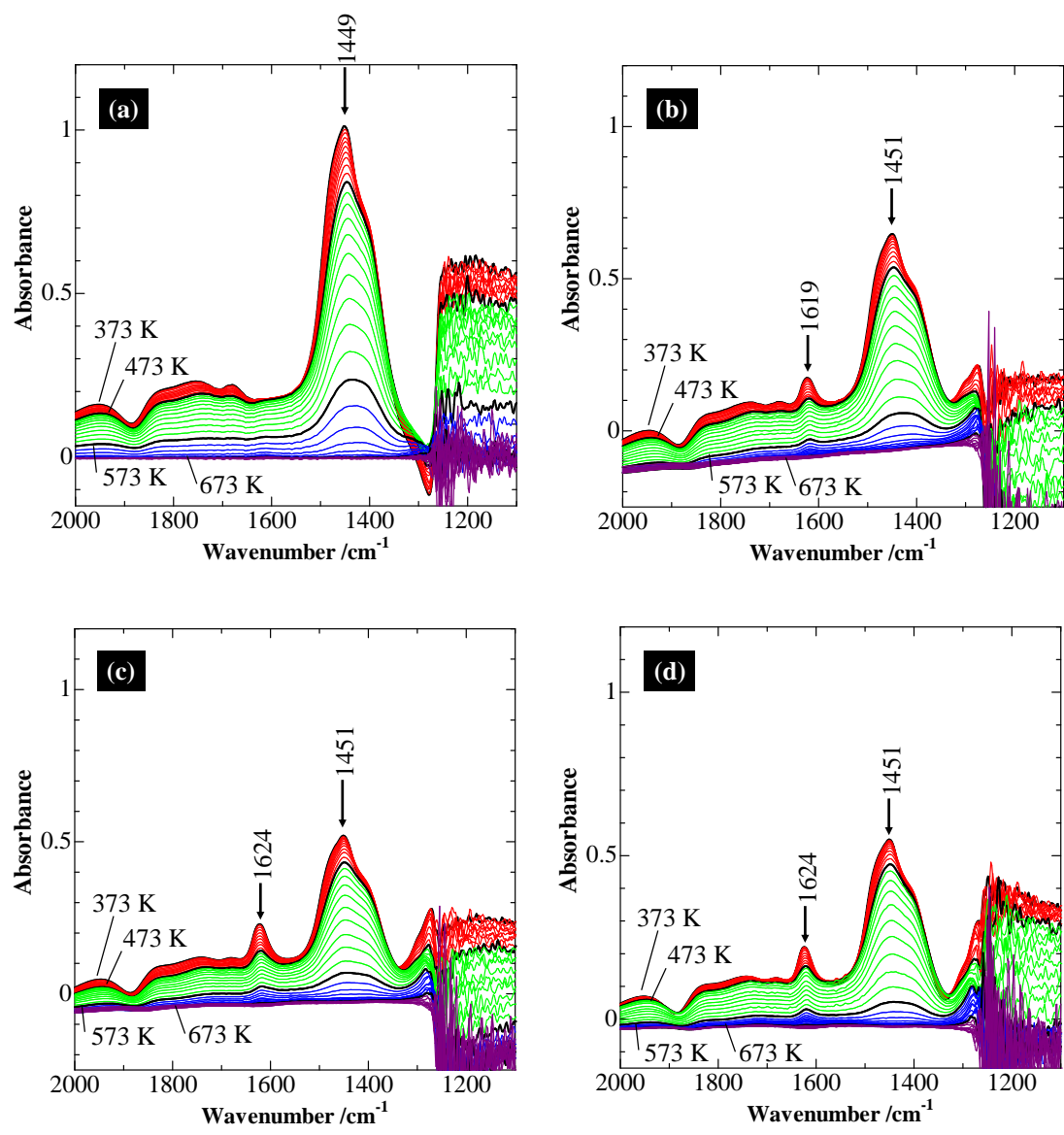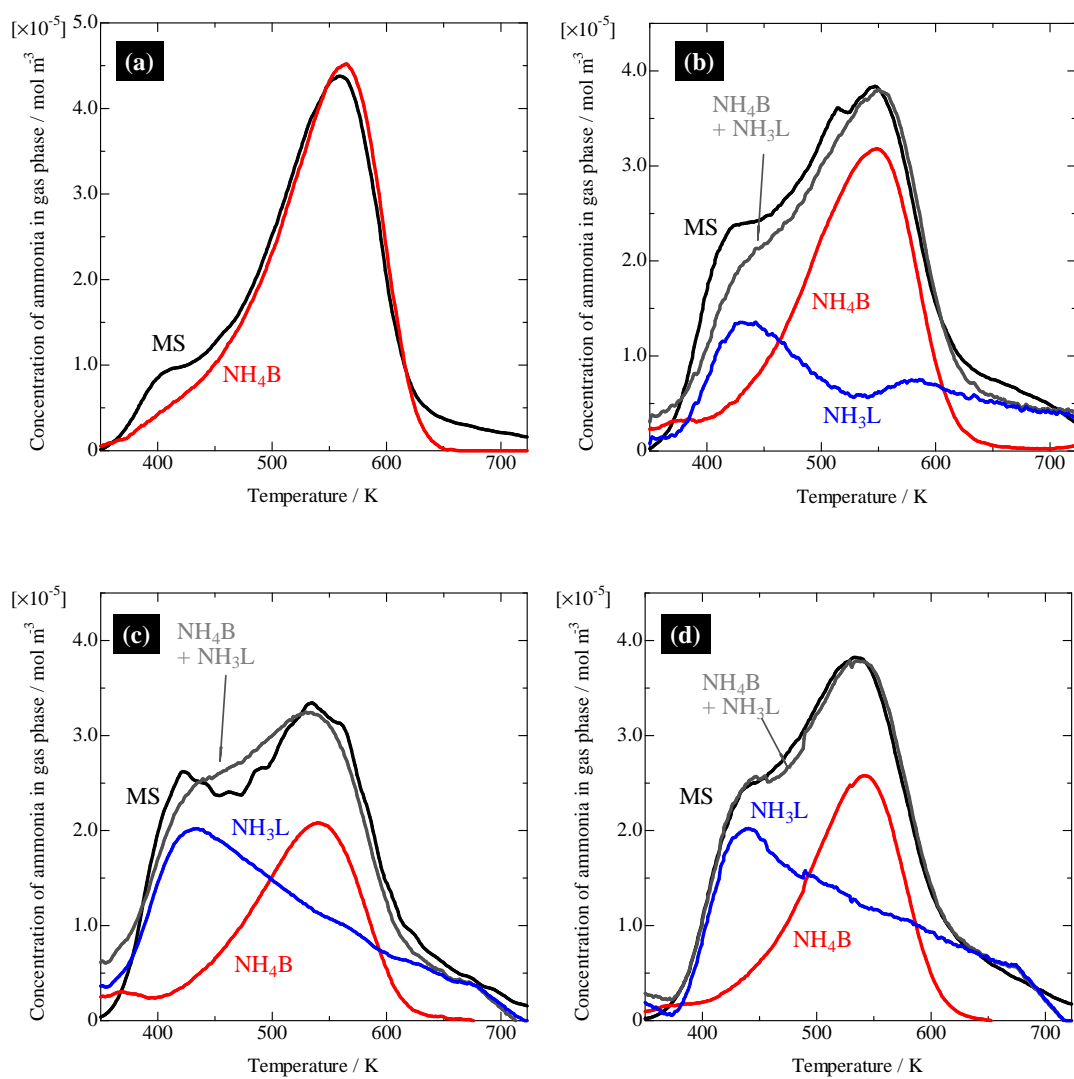
Fig. 1
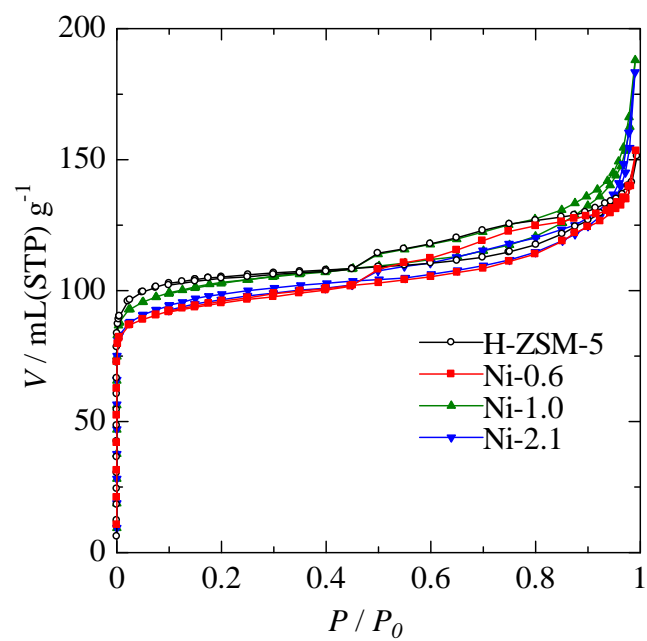
Fig. 2

Fig. 3

Fig. 4

Fig. 5

Fig. 6

Fig. 7